

WHY MASSIVE BLACK HOLES ARE SMALL IN DISK GALAXIES ?

NOZOMU KAWAKATU¹ AND MASAYUKI UMEMURA²Center for Computational Physics, University of Tsukuba, Ten-nodai, 1-1-1 Tsukuba, Ibaraki, 305-8577,
Japan*Draft version December 1, 2018*

ABSTRACT

A potential mechanism is proposed to account for the fact that supermassive black holes (SMBHs) in disk galaxies appear to be smaller than those in elliptical galaxies in the same luminosity range. We consider the formation of SMBHs by radiation drag (Poynting-Robertson effect), which extracts angular momentum from interstellar matter and thereby drives the mass accretion onto a galactic center. In particular, we quantitatively scrutinize the efficiency of radiation drag in a galaxy composed of bulge and disk, and elucidate the relation between the final mass of SMBH and the bulge-to-disk ratio of the galaxy. As a result, it is found that the BH-to-galaxy mass ratio, $M_{\text{BH}}/M_{\text{galaxy}}$, decreases with a smaller bulge-to-disk ratio, due to the effects of geometrical dilution and opacity, and is reduced maximally by two orders of magnitude, resulting in $M_{\text{BH}}/M_{\text{galaxy}} \approx 10^{-5}$. In contrast, if only the bulge components in galaxies are focused, the BH-to-bulge mass ratio becomes $M_{\text{BH}}/M_{\text{bulge}} \approx 10^{-3}$, which is similar to that found in elliptical galaxies. Thus, it turns out that the mass of SMBH primarily correlates with a bulge, not with a disk, consistently with observational data.

Subject headings: black hole physics — galaxies:active — galaxies:disk — galaxies:nuclei — galaxies:starburst

1. INTRODUCTION

Supermassive black holes (SMBHs) are now thought to reside in virtually all galactic bulges. The recent compilation of the kinematical data of galactic centers in both active and inactive galaxies has shown that the mass of SMBH does correlate with the mass of a galactic bulge; the mass ratio of BH to bulge is ≈ 0.001 as a median value (Kormendy & Richstone 1995; Richstone et al. 1998; Magorrian et al. 1998; Gebhardt et al. 2000; Ferrarese & Merritt 2000; Merritt & Ferrarese 2001; McLure & Dunlop 2001, 2002; Wandel 2002). On the other hand, it appears that the SMBH does not correlate with a disk component (Kormendy & Gebhardt 2001). In disk galaxies, the mass ratio is significantly smaller than 0.001 if disk stars are included (Salucci et al. 2000; Sarzi et al. 2001, Ferrarese 2002, Baes et al. 2003). These observations imply that the formation of the SMBH is related to the bulge components of galaxies.

Recently, as a possible mechanism for the formation of SMBHs, the radiation-hydrodynamic model is proposed, where the radiation drag (Poynting-Robertson effect) due to stellar radiation in a galactic bulge drives the mass accretion to grow a massive BH (Umemura 2001). This is a parallel model of the formation of massive BHs by the Compton drag in an early universe (Umemura, Loeb, & Turner 1997). In an optically thick regime, the efficiency of radiation drag is saturated due to the conservation of the photon number (Tsuribe & Umemura 1997). The timescale of radiation drag-induced mass accretion is $t_{\text{drag}} = 8.6 \times 10^7 R_{\text{kpc}}^2 (L_*/10^{12} L_\odot)^{-1} (Z/Z_\odot)^{-1} \text{yr}$, where R_{kpc} is the galaxy size in units of kpc, and Z is the metallicity of gas. The mass accretion rate is given by $\dot{M} = -M_g d \ln J/dt \simeq L_*/c^2$, where J , L_* , and M_g are the

total angular momentum of gaseous component, the total luminosity of the system, and the total mass of gas, respectively. Thus, the final BH mass is estimated by $M_{\text{BH}} \simeq \int L_*(t)/c^2 dt$. Hence, the final BH mass is proportional to the total radiation energy from stars, and the theoretical upper limit of BH-to-bulge mass ratio is determined by the energy conversion efficiency of nuclear fusion from hydrogen to helium, i.e., 0.007 (Umemura 2001). In practice, the inhomogeneity of interstellar medium helps the radiation drag to sustain high efficiency (Kawakatu & Umemura 2002). By incorporating the realistic chemical evolution, the radiation drag model predicts $M_{\text{BH}}/M_{\text{bulge}} \simeq 0.001$ (Kawakatu, Umemura, & Mori 2003). However, the radiation drag efficiency could be strongly subject to the effect of geometry (Umemura et al. 1997, 1998; Ohsuga et al. 1999a). If the system is spherical, the emitted photons are effectively consumed within the system, whereas a large fraction of photons can escape from disk-like systems, and thus the drag efficiency is likely to be reduced considerably. It is suggested that such a geometrical effect may be the reason why the BH is smaller in disk galaxies (Umemura 2001; Umemura 2003), although the details have not been clear quantitatively.

In this Letter, we scrutinize the efficiency of radiation drag in a system composed of bulge and disk. For the purpose, we accurately solve the 3D radiative transfer in an inhomogeneous interstellar medium. The main goal is to elucidate the relationship between the final BH mass formed by the radiation drag and the bulge-to-disk ratio of host galaxy.

2. MODEL

We consider a system composed of bulge and disk, which consist of dark matter, stars, and dusty interstellar mat-

¹ kawakatu@rccp.tsukuba.ac.jp² umemura@rccp.tsukuba.ac.jp

ter (ISM). The total baryonic mass of the system, M_b , is set to be $10^{11}M_\odot$. But, it is noted that the results are scaled with M_b . The dark matter is distributed following the profile by Navarro, Frenk, & White (1997), $\rho(r) \propto (r/r_s)^{-1}(1+r/r_s)^{-2}$, where r_s is the characteristic radius, which is $r_s = 50\text{kpc}$ here. The mass of the dark matter component, M_{DM} , is equal to M_b within the galaxy size of $r_g = 10\text{kpc}$.

We incorporate the evolution of galaxy from the formation stage, where a galactic system starts with a protogalactic cloud purely composed of baryonic gas. By invoking the star formation in Schmidt's law, stellar components are generated in this system. To include the recycling of ISM, we employ an evolutionary spectral synthesis code, PEGASE (Fioc & Rocca-Volmerange 1997), with assuming a Salpeter-type initial mass function (IMF) as $\phi = dn/d\log m_* = \phi_0(m_*/M_\odot)^{-1.35}$ for the mass range of $[0.1M_\odot, 60M_\odot]$, where m_* is the stellar mass. The star formation rate (SFR) per unit mass at time t , $C(t)$, is assumed to be proportional to the gas mass fraction, $C(t) = kf_g$ with $f_g \equiv M_g(t)/M_b$, where k is a rate coefficient which is 8.6Gyr^{-1} for the bulge component and 0.86Gyr^{-1} for the disk component, respectively.

The formed stars in the bulge are distributed following Hernquist's profile (1990), which mimics de Vaucouleur's profile: $\rho(r) \propto (r/r_{\text{core}})^{-1}(1+r/r_{\text{core}})^{-3}$, where r_{core} is the core radius. The bulge radius, r_{bulge} , is given by a mass-to-size relation as $r_{\text{bulge}}/r_g = (M_{\text{bulge}}/M_{\text{galaxy}})^{1/2}$ (Kormendy 1985; Chiosi & Carraro 2002), where M_{bulge} is the bulge mass and M_{galaxy} is the final stellar mass of the galaxy, and r_{core} is set to $r_{\text{core}} = 0.1r_{\text{bulge}}$. In the present analysis, the bulge mass fraction ($M_{\text{bulge}}/M_{\text{galaxy}}$) is altered as a key parameter. In addition, angular momentum is smeared, assuming rigid rotation, according to the spin parameter of $\lambda = 0.05$ (Barnes & Efstathiou 1987; Heavens & Peacock 1988).

As for the disk component, formed stars are distributed exponentially in the radial direction, with assuming the vertical scale-height which is changed from $0.01r_g$ to $0.1r_g$. The disk radius, r_{disk} , is given by a mass-to-size relation of $r_{\text{disk}}/r_g = (M_{\text{disk}}/M_{\text{galaxy}})^{1/2}$, where M_{disk} is the disk mass. The disk component is assumed to be in rotation balance.

As for ISM, we consider clumpy matter, since the ISM is observed to be highly inhomogeneous in active star-forming galaxies (Sanders et al. 1988; Gordon, Calzetti, & Witt 1997). Here, $N_c (= 10^4)$ identical clouds are distributed randomly in a system of the bulge and disk. The number of clouds is minimal enough to resolve the disk scale-height of $0.01r_g$. (It is noted that simulations with a three times larger number of clouds did not lead to any fundamental difference.) The distribution and motion of the ISM is the same as those of stellar components. We assume that the cloud covering factor is unity according to the analysis by Kawakatu & Umemura (2002). The internal density in a cloud is assumed to be uniform, and the opacity is determined by a dust-to-gas ratio which is calculated by PEGASE. The optical depth of a cloud and therefore the overall optical depth of galaxy, τ_T , depend on the cloud size r_c , where $r_c = 100\text{pc}$ is assumed as a fiducial case. But we have confirmed that no essential difference in the final BH mass is found by changing r_c so as

to enhance τ_T by an order.

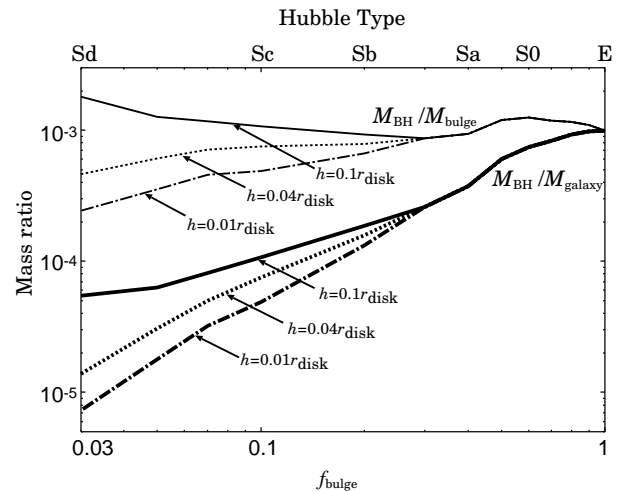


FIG. 1.— The BH-to-galaxy mass ratio ($M_{\text{BH}}/M_{\text{galaxy}}$) and the BH-to-bulge mass ratio ($M_{\text{BH}}/M_{\text{bulge}}$) are shown against the bulge fraction, $f_{\text{bulge}} \equiv M_{\text{bulge}}/M_{\text{galaxy}}$. The thick lines show $M_{\text{BH}}/M_{\text{galaxy}}$ with changing the disk scale-height from $h = 0.01r_{\text{disk}}$ up to $h = 0.1r_{\text{disk}}$ and the thin lines do $M_{\text{BH}}/M_{\text{bulge}}$. The top abscissa is the indication for the Hubble type, which is determined by the mean bulge-to-disk ratio for disk galaxies (Kent 1985).

The radiation drag, which drives the mass accretion, originates in the relativistic effect in absorption and re-emission of radiation. This effect is involved in relativistic radiation hydrodynamics (RHD) (Umemura, Fukue, & Mineshige 1997, 1998; Fukue, Umemura, & Mineshige 1997). The angular momentum transfer in RHD is given by the azimuthal equation of motion in cylindrical coordinates,

$$\frac{1}{r} \frac{d(rv_\phi)}{dt} = \frac{\chi}{c} [F^\phi - (E + P^{\phi\phi})v_\phi], \quad (1)$$

where χ is the mass extinction coefficient, E is the radiation energy density, F^ϕ is the radiation flux, and $P^{\phi\phi}$ is the radiation stress tensor. All radiative quantities are determined by radiation from stars diluted by dusty ISM. Here, we solve radiative transfer including the dust extinction by ISM and obtain these radiative quantities. Then, we evaluate the total angular momentum loss rate (see Kawakatu & Umemura 2002 for the details of method). If an optically thick cloud is irradiated by the radiation, an optically-thin surface layer is stripped by the radiation drag (Tsuribe & Umemura 1997), and loses angular momentum. Since the bulge luminosity is lower than the Eddington luminosity for dusty gas, $L_{\text{Edd}} = 4\pi cGM_{\text{dyn}}/\chi$ with the dynamical mass M_{dyn} within r_g , during the whole history of galaxy, the stripped gas is not blown away by the radiation pressure, but confined in the galaxy. Hence, the gas moves in a gravitational potential weakened by radiation pressure and loses angular momentum by radiation drag. The stripped gas losing angular momentum falls onto the galactic center to form a massive object, which is likely to undergo the inside-out viscous collapse (Mineshige, Tsuribe, & Umemura 1998; Tsuribe 1999) and eventually evolve into a SMBH by the general relativistic instability (Saijo et al. 2002; Shibata & Shapiro 2002). Using equation (1), we can calculate the mass accretion rate onto the central object by $\dot{M}_g/M_g = -\dot{J}/J$, where

J is the total angular momentum of ISM. Then, the BH mass (M_{BH}) is assessed as

$$M_{\text{BH}} = \int_0^{t_0} \dot{M}_g dt = - \int_0^{t_0} M_g \frac{\dot{J}}{J} dt, \quad (2)$$

where t_0 is the Hubble time.

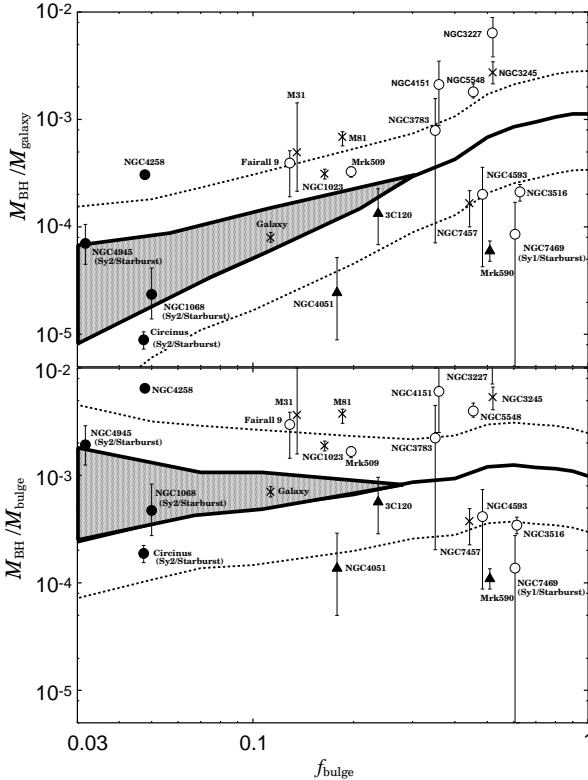


FIG. 2.— Comparison between the theoretical prediction and the observational data on BH mass for disk galaxies. The upper panel shows the BH-to-galaxy mass ratio ($M_{\text{BH}}/M_{\text{galaxy}}$) and the lower panel shows the BH-to-bulge mass ratio ($M_{\text{BH}}/M_{\text{bulge}}$) against the bulge fraction, $f_{\text{bulge}} \equiv M_{\text{bulge}}/M_{\text{galaxy}}$. The observational data are based upon Table 1 and plotted by symbols: *Crosses* – disk galaxies which do not possess AGNs, *open circles* – Seyfert 1 galaxies (Sy1s), *filled triangles* – narrow line Seyfert 1 galaxies (NLSy1s), and *filled circles* – Seyfert 2 galaxies (Sy2s). Seyfert galaxies accompanied by starburst activities are specified like Sy1/starburst or Sy2/starburst. The hatched area is the prediction shown in Fig. 1. Two dotted lines in each panel are the upper and lower bound of the theoretical prediction by including uncertainties other than the geometrical effect (see the end of §3).

3. RESULTS

By changing the bulge mass fraction, $f_{\text{bulge}} \equiv M_{\text{bulge}}/M_{\text{galaxy}}$, we investigate the relation between the final BH mass and the bulge-to-disk ratio of galaxy. The growth of BH depends upon the optical depth of galaxy, τ_{T} , but no essential difference in the final BH mass is found by enhancing τ_{T} by an order, because the mass accretion rate is saturated when the system becomes optically-thick (Umemura 2001; Kawakatu & Umemura 2002). In Figure 1, the resultant BH-to-galaxy mass ratio, $M_{\text{BH}}/M_{\text{galaxy}}$, is shown against the bulge mass fraction (f_{bulge}) by thick lines for three values of disk scale-height. We can see a clear trend that $M_{\text{BH}}/M_{\text{galaxy}}$ decreases with decreasing f_{bulge} . This tendency comes from three effects: First, a larger number of photons escape from the disk surface, since the surface-to-volume ratio is larger for the disk com-

ponent compared to the bulge. This effect is called the *geometrical dilution* here. Secondly, the radiation from disk stars is heavily diminished across the disk, because the edge-on optical depth becomes larger quickly. Thirdly, the velocity difference between a star and an absorbing cloud becomes closer to zero in an optically-thick disk, so that the radiation drag cannot work effectively. For instance, if $f_{\text{bulge}} = 0.03$ which corresponds to Sd galaxies, $M_{\text{BH}}/M_{\text{galaxy}}$ is reduced by a factor of ≈ 20 to ≈ 100 , compared to $M_{\text{BH}}/M_{\text{galaxy}} \approx 0.001$ for elliptical galaxies ($f_{\text{bulge}} = 1$). Furthermore, it is predicted that a bulgeless (pure disk) system can also possess a massive black hole with the mass ratio of $M_{\text{BH}}/M_{\text{galaxy}} \simeq 0.001 \times (h/2r_{\text{disk}})$, where h is the scale height of disk. This ranges from 6×10^{-6} to 5×10^{-5} , corresponding to $h = 0.01r_{\text{disk}}$ and $h = 0.1r_{\text{disk}}$, respectively.

On the other hand, the bulge component itself is likely to be impervious to the above three geometrical effects. In Figure 1, by focusing on only the bulge component, the BH-to-bulge mass ratio, $M_{\text{BH}}/M_{\text{bulge}}$, is also shown. As seen in Figure 1, $M_{\text{BH}}/M_{\text{bulge}}$ is almost constant as expected. Hence, it is concluded that the BH-to-galaxy mass ratio in disk galaxies is substantially determined by bulge components, not by disk components: $M_{\text{BH}}/M_{\text{galaxy}} \simeq 0.001$, where the constant value of 0.001 is basically determined by the energy conversion efficiency of nuclear fusion from hydrogen to helium, i.e., 0.007 (Umemura 2001). The BH accretion can trigger an active galactic nucleus (AGN) as well, and then the further mass accretion is induced via radiation drag by the AGN. The effect can enhance the final BH mass maximally by a factor of 1.7 (Umemura 2001). Also, a different level of ISM clumpiness can reduce the final BH mass by a factor of 2 (Kawakatu & Umemura 2002). As for the effect of IMF, if the slope and the mass range of IMF are changed to satisfy the spectrophotometric properties, then the final BH mass is altered by a factor of $\pm 40\%$. Similar uncertainties attach also to the final BH mass in disk galaxies.

4. COMPARISON WITH OBSERVATIONS

The present results are compared with observational data for SMBHs in disk galaxies in Figure 2. The data we adopted are summarized in Table 1. In the upper panel of Figure 2, $M_{\text{BH}}/M_{\text{galaxy}}$ is shown against f_{bulge} . The hatched area is the prediction shown in Figure 1. Two dotted lines are respectively the upper and lower bound of the prediction by including other theoretical uncertainties mentioned above. The observational data are categorized into four types: disk galaxies which do not possess AGNs, Seyfert 1 galaxies (Sy1s), narrow line Seyfert 1 galaxies (NLSy1s), and Seyfert 2 galaxies (Sy2s). Also, the objects accompanied with starburst events are specified. The observational data in Figure 2 shows the decrease of $M_{\text{BH}}/M_{\text{galaxy}}$ by more than an order of magnitude from $f_{\text{bulge}} = 1$ to $f_{\text{bulge}} = 0.03$. This trend is broadly consistent with the theoretical prediction. But, it is worth noting that several objects possess relatively small BHs compared to the prediction, and they are mostly Seyfert galaxies with starburst events (NGC 7469, NGC 1068, Circinus) or NLSy1s (Mrk 590, NGC 4051). In recent years, an evolutionary model for AGNs beyond the AGN unified theory has been considered from both observational and theo-

retical points of view (Maiolino et al. 1995; Radovich, Rafanelli, & Barbon 1998; Ohsuga & Umemura 1999, 2001). In this model, AGNs with starbursts are in earlier evolutionary phase, and therefore the BH mass is likely to be smaller, compared to a post-starburst phase. Furthermore, NLSy1s are thought to be in a rapidly growing phase of an immature BH (Mathur et al. 2001). NGC1068 could be also in such a phase (Kawaguchi 2003). This point may be intriguing to analyze further with larger sample data in the future.

In the lower panel of Figure 2, $M_{\text{BH}}/M_{\text{bulge}}$ is shown against f_{bulge} . When only the bulge component is focused, the observational data for $M_{\text{BH}}/M_{\text{bulge}}$ lies at a level of ≈ 0.001 , and they roughly agree with the prediction. But, again the ratios for Seyferts with starbursts and NLSy1s

fall appreciably below 0.001.

The present model also predicts a SMBH even in a pure disk system without bulge, and the mass of BH depends upon the disk scale-height. NGC4395 is an archetype of bulgeless galaxy in which a massive BH resides (Filipenko & Ho 2003). The BH fraction in this galaxy is estimated to be $M_{\text{BH}}/M_{\text{galaxy}} \simeq 1.5 \times 10^{-5}$. In the present model, this level can be realized by a disk scale height of $h \approx 0.04r_{\text{disk}}$.

We thank T.Nakamoto, T.Saitou and A.Yonehara for helpful discussions. We also thank the anonymous referee for precious comments. Numerical simulations were performed with facilities at the Center of Computational Physics, University of Tsukuba. This work was supported in part by the Grant-in-Aid of the JSPS, 11640225.

REFERENCES

- Baes, M., et al. 2003, MNRAS, MNRAS, 341, L44
 Barnes, J., & Efstathiou, G. 1987, ApJ, 319, 575
 Barth, R., et al. 2001, ApJ, 555, 685
 Bender, R. 2003, ApJ, submitted
 Bower, G.A., et al. 2000, BAAS, 32, 1566
 Bower, G.A., et al. 2001, ApJ, 550, 75
 Chiosi, C., & Carraro, G., MNRAS, 2002, 335, 335
 Ferrarese, L. 2002, ApJ, 578, 90
 Ferrarese, L., & Merritt, D. 2000, ApJ, 539, L9
 Filippenko, A.V., & Ho, L.C. 2003, ApJ, 588, L13
 Fioc, M., & Rocca-Volmerrange, B. 1997, A&A, 326, 950
 Fukue, J., Umemura, M., & Mineshige, S. 1997, PASJ, 49, 673
 Gebhardt, K., et al. 2000, ApJ, 543, L5
 Gebhardt, K., et al. 2003, ApJ, 583, 92
 Gordon, K., Calzetti, D., & Witt, A.N. 1997, ApJ, 487, 625
 Greenhill, L.J., et al. 1996, ApJ, 472, L21
 Greenhill, L.J., et al. 1997, ApJ, 481, L23
 Greenhill, L.J., et al. 2003, ApJ, 590, 162
 Heaveans, A., & Peacock, J. 1988, MNRAS, 232, 339
 Hernquist, L. 1990, ApJ, 356, 359
 Kawaguchi, T. 2003, ApJ, 593, 69
 Kawakatu, N., Umemura, M., & Mori, M. 2003, ApJ, 583, 85
 Kawakatu, N., & Umemura, M. 2002, MNRAS, 329, 572
 Kent, S.M., 1985, ApJS, 59, 115
 Kormendy, J., & Gebhardt, K. 2001, in The 20th Texas Symposium on Relativistic Astrophysics, ed. H.Martel & J.C.Wheeler (Melville: AIP), 363
 Kormendy, J., & Richstone, D. 1995, ARA&A, 33, 581
 Kormendy, J., 1985, ApJ, 295, 73
 Magorrian, J., et al. 1998, AJ, 115, 2285
 Maiolino, R., Ruiz, M., Rieke, G. H., & Keller, L. D. 1995, ApJ, 446, 561
 Mathur, S., Kuraszkiewicz, J., & Czerny, B., 2001, New Astronomy, 6, 321
 McLure, R.J., & Dunlop, J.S. 2001, MNRAS, 327, 199
 McLure, R.J., & Dunlop, J.S. 2002, MNRAS, 331, 795
 Merritt, D., & Ferrarese, L. 2001, MNRAS, 320, L30
 Mineshige, S., Tsuribe, T., & Umemura, M. 1998, PASJ, 50, 233
 Miyoshi et al. 1995, Nature, 373, 127
 Navarro, J.F., Frenk, C.S., & White, S.D.M. 1997, ApJ, 490, 493
 Ohsuga, K., & Umemura, M. 2001, ApJ, 559, 157
 Ohsuga, K., Umemura, M., Fukue, J., & Mineshige, S. 1999a, PASJ, 51, 345
 Ohsuga, K., & Umemura, M. 1999b, ApJ, 521, L13
 Onken et al. 2003, ApJ, 585, 121
 Radovich, M., Rafanelli, P., & Barbon, R. 1998, A&A, 334, 124
 Richstone, D., et al. 1998, Nature, 395A, 14
 Saijo, M., Baumgarte, T.W., Shapiro, S.L., & Shibata, M. 2002, ApJ, 569, 349
 Salucci, P., et al. 2000, MNRAS, 317, 488
 Sanders, D.B., et al. 1988, ApJS, 325, 74
 Sarzi, M., et al. 2001, ApJ, 550, 65
 Schödel, R., et al. 2002, Nature, 419, 694
 Shibata, M., & Shapiro, S. 2002, 572, L39
 Tsuribe, T. 1999, ApJ, 527, 102
 Tsuribe, T., & Umemura, M. 1997, ApJ, 486, 48
 Umemura, M. 2003, Coevolution of Black Holes and galaxies, ed. L.C.Ho (Pasadena: Carnegie Observatories)
 Umemura, M. 2001, ApJ, 560, L29
 Umemura, M., Fukue, J., & Mineshige, S. 1998, MNRAS, 299, 1123
 Umemura, M., Fukue, J., & Mineshige, S. 1997, ApJ, 479, L97
 Umemura, M., Loeb, A., & Turner, E. L. 1993, 419, 459
 Wandel, A. 1999, ApJ, 519, L39
 Wandel, A. 2002, ApJ, 565, 762

Table 1. SMBHs in Disk Galaxies

Object	Type	$M_{\text{galaxy}}(M_{\odot})$	$M_{\text{bulge}}(M_{\odot})$	$M_{\text{BH}}(M_{\odot})$	AGN	Starburst	Reference
Galaxy	Sbc	4.6×10^{10}	5.2×10^9	$3.7(\pm 0.4) \times 10^6$	—	—	1
M31	Sb	1.4×10^{11}	1.9×10^{10}	$7(+13 - 4) \times 10^7$	—	—	2
M81	Sb	9.7×10^{10}	1.8×10^{10}	$6.8(+0.7 - 1.3) \times 10^7$	—	—	3
NGC1023	SB0	1.4×10^{11}	2.3×10^{10}	$4.4(+0.4 - 0.5) \times 10^7$	—	—	4
NGC3245	S0	7.5×10^{10}	3.9×10^{10}	$2.1(\pm 0.5) \times 10^8$	—	—	5
NGC7457	S0	2.1×10^{10}	9.3×10^9	$3.5(+1.1 - 1.4) \times 10^6$	—	—	6
Fairall 9	S	2.2×10^{11}	2.9×10^{10}	$8.7(+2.6 - 4.5) \times 10^7$	Sy1	—	7
Mrk509	S	2.9×10^{11}	5.7×10^{10}	$9.5(+1.1 - 1.1) \times 10^7$	Sy1	—	7
NGC3516	SB0	8.0×10^{10}	4.9×10^{10}	$1.7(\pm 0.3) \times 10^7$	Sy1	—	8
NGC3783	SBa	1.4×10^{10}	4.9×10^9	$1.1(+1.1 - 1.0) \times 10^7$	Sy1	—	7
NGC4151	SA	5.7×10^9	2.0×10^9	$1.2(+0.8 - 0.7) \times 10^7$	Sy1	—	7
NGC3227	SAa	5.6×10^9	2.9×10^9	$3.6(\pm 1.4) \times 10^7$	Sy1	—	8
NGC4593	SBb	3.3×10^{10}	1.6×10^{10}	$6.6(\pm 5.2) \times 10^6$	Sy1	—	8
NGC5548	Sa	4.4×10^{10}	2.0×10^{10}	$8.0(+1.5 - 1.0) \times 10^7$	Sy1	—	7
NGC7469	SA	8.9×10^{10}	5.5×10^{10}	$7.6(+7.5 - 7.6) \times 10^6$	Sy1	Nuclear	7
3C120	S0	2.2×10^{11}	5.2×10^{10}	$3.0(+2.0 - 1.5) \times 10^7$	NLSy1	—	7
Mrk590	Sa	2.3×10^{11}	1.1×10^{11}	$1.4(+0.3 - 0.3) \times 10^7$	NLSy1	—	7
NGC4051	SB	5.6×10^{10}	1.1×10^{10}	$1.4(+1.5 - 0.9) \times 10^6$	NLSy1	—	7
Circinus	Sb-Sd	1.9×10^{11}	9.0×10^9	$1.7(\pm 0.3) \times 10^6$	Sy2	Nuclear	9
NGC1068	Sb	7.2×10^{11}	3.6×10^{10}	$1.7(+1.3 - 0.7) \times 10^7$	Sy2	Circumnuclear	10
NGC4258	Sbc	1.3×10^{11}	6.2×10^9	$4.0(\pm 0.1) \times 10^7$	Sy2	—	11
NGC4945	Scd	2.4×10^{10}	7.2×10^8	$1.4(+0.7 - 0.5) \times 10^6$	Sy2	Nuclear	12

References: 1) Schödel et al. 2003, 2) Bender et al. 2003, 3) Bower et al. 2000, 4) Bower et al. 2001, 5) Barth et al. 2001, 6) Gebhardt et al. 2003, 7) Wandel 1999, 8) Onken et al. 2003, 9) Greenhill et al. 2003, 10) Greenhill et al. 1996, 11) Miyoshi et al. 1995, 12) Greenhill et al. 1997